PHYSICAL REVIEW B VOLUME 33, NUMBER 2 15 JANUARY 1986

Transient photovoltaic effect in semiconductor superlattices

J. A. Brum, P. Voisin, and G. Bastard
Groupe de Physique des Solides de l'Ecole Normale Supérieure, 24 rue Lhomond, 75231 Paris Cédex 05, France
(Received 3 June 1985)

We present a quantum theory of the transient photovoltaic effect which occurs in sawtooth and InAs-GaSb superlattices. This effect arises from the lack of reflection symmetry and from the carrier spatial separation. The ground-state eigenfunctions and the electronic structure of sawtooth superlattices are obtained with use of the envelope-function method. Finally, we discuss the time dependence of this new photovoltaic effect.

During the last few years, heterostructures and superlattices have been intensively studied both for their novel physical properties and for device applications. Recently, attention was paid to multilayer graded-gap structures (sawtooth superlattices) as an interesting material for device applications. More specifically, Capasso *et al.*[1] proposed a new type of photodetector using a sawtooth superlattice structure. Their idea is based on the lack of inversion symmetry and the spatial separation of the photocarriers occuring in these structures. They performed experiments consisting of the detection of a voltage pulse induced by a short light pulse across the sawtooth superlattice. They observed a transient voltage of about 10 mV with a decay time $\tau \approx 200$ ps.

Spatial separation of electrons and holes does not occur only in sawtooth superlattices. Type-II superlattices, such as InAs-GaSb, also display this property, since the electrons are confined in one layer and the holes in the other. We thus expect equivalent transient photovoltaic effects in these structures. In the same way "*nipi*" superlattices should exhibit a similar behavior. In all these structures, the photoinjected electrons and holes spatially separate when thermalizing towards their respective band extrema, which occurs on a subpicosecond time scale.[2] The accurate description of the quantum ground state is thus essential to the understanding of the present effect. In this paper, we report a theoretical study of the transient photovoltaic effect in both sawtooth and type-II superlattices and discuss briefly the case of *nipi* structures.

We calculate first the band structure and eigenfunctions of sawtooth superlattices. The graded Al concentration creates a potential which is similar to an external electric field potential (Fig. 1) with the difference that it concentrates the carriers on the same side of the heterointerface in both the valence and conduction bands.

This potential, when periodic, gives a subband structure in the growth direction z. As we are interested only in a qualitative description, we use a simplified version of the envelope-function approximation[3] to calculate these subband energies. We neglect the nonparabolicity of the bands, and we consider the case $k_\perp = (k_x, k_y) = 0$. The alloy medium of varying aluminum concentration is taken as an effective medium. We thus describe the system by a scalar Hamiltonian, corresponding to decoupled bands:

$$H\psi = \left[\frac{-\hbar^2}{2m^*} \frac{d^2}{dz^2} + V_b \frac{z}{d} \right] \psi = E\psi \,, \quad nd \leq z \leq (n+1)d, \quad n = 0,1,2 \tag{1}$$

where d is the periodicity of the superlattice, V_b is the conduction- (valence-) band maximum discontinuity, and m^* is the effective mass of the conduction- (valence-) band effective medium. As boundary conditions at the abrupt interface, we impose the continuity of the function and of the density of probability current.

The periodic potential gives an additional condition expressed by the Bloch theorem:

$$\psi(z+nd) = e^{iqnd}\psi(z) \,. \tag{2}$$

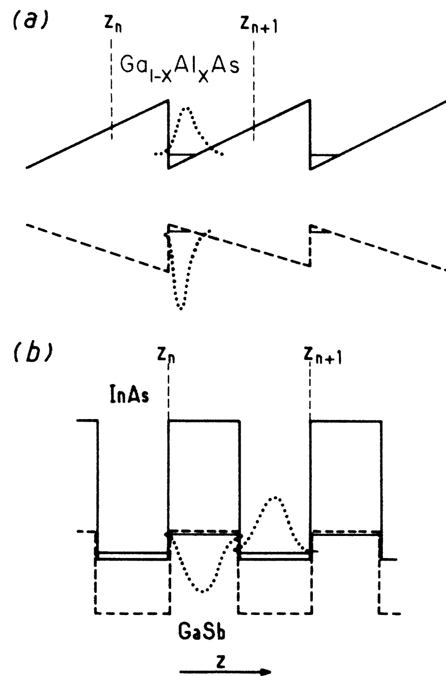

FIG. 1. Conduction- and valence-band profiles in (a) a sawtooth superlattice and (b) a type-II InAs-GaSb superlattice. The squared wave-function amplitudes for the ground states in each band are also shown.

 ©1986 The American Physical Society

The eigenfunctions are obtained as a linear combination of the independent Airy functions A_i and B_i:

$$\psi(z)=\alpha A_i[x(z)]+\beta B_i[x(z)],\quad 0\leq z\leq d \tag{3a}$$

and

$$\psi(z)=aA_i[x(z-d)]+bB_i[x(z-d)],\quad d\leq z\leq 2d \tag{3b}$$

where

$$x(z)=\left[\frac{\hbar^2 d}{2m^* V_b}\right]^{-1/3}\left[z-\frac{E}{V_b}d\right]. \tag{4}$$

By matching $\psi(z)$ and $d\psi/dz$ at the interfaces $z=0$ and $z=d$, we readily obtain the dispersion relation:

$$\begin{aligned}2W_0\cos(qd)= {} & A_i[x(0)]\frac{d}{dz}B_i[x(z)]\Big|_{z=d} \\ & +A_i[x(d)]\frac{d}{dz}B_i[x(z)]\Big|_{z=0} \\ & -\frac{d}{dz}A_i[x(z)]\Big|_{z=d}B_i[x(0)] \\ & -\frac{d}{dz}A_i[x(z)]\Big|_{z=0}B_i[x(d)],\end{aligned} \tag{5}$$

where

$$W_0= A_i[x(d)]\frac{d}{dz}B_i[x(z)]\Big|_{x=d} - B_i[x(d)]\frac{d}{dz}A_i[x(z)]\Big|_{z=d}. \tag{6}$$

The subband energies and bandwidths are calculated for electrons and holes as a function of the period for a maximum Al concentration, $x_{\max}=0.2$. The effective masses of the effective alloy medium are taken equal to those of bulk GaAs: $m_e=0.067m_0$ for the conduction band (CB), $m_{\rm hh}=0.45m_0$ for the heavy-hole valence band (VB), and $m_{\rm lh}=0.08m_0$ for the light-hole valence band. The band offsets used are 60% and 40% of the band-gap difference for the conduction and valence bands, respectively.[4] The results are shown in Fig. 2.

For $d>250$ Å, the conduction ground subbands are practically dispersionless, reflecting the absence of overlap between wave functions of neighboring cells. The heavy-hole subbands remain essentially flat for periods larger than 150 Å. These results are to be compared to those obtained by Jaros *et al.*[5], who calculated the band structure of sawtooth superlattices using a nonlocal pseudopotential method. Significant discrepancies are worth noting: first, the ground conduction subband minimum is always at the superlattice zone center and not away from it as it appears from their calculations; second, for a superlattice period of 140 Å and $x_{\max}$ of 0.3, they found a conduction ground state essentially dispersionless ($\Delta E\approx 1$ meV). Using their parameters, our calculation gives a subband width of about 8 meV. We believe that the simplifications done in the present work cannot explain these discrepancies which, anyway, should not affect the following.

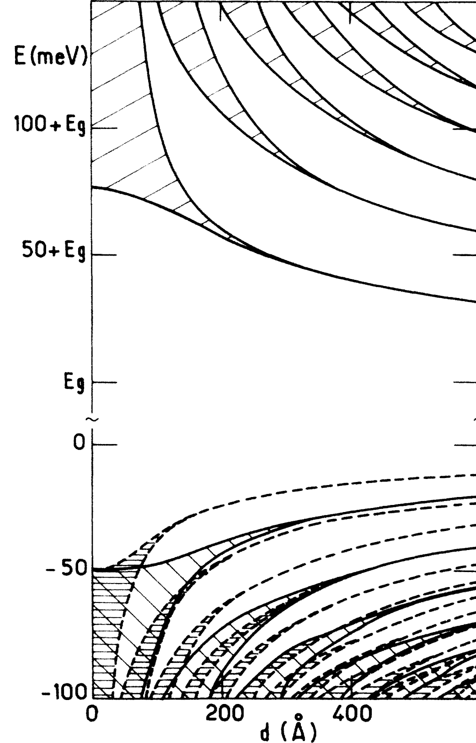

FIG. 2 Calculated subband energies and bandwidths for electrons and heavy and light holes as a function of the period in a GaAs-$\text{Ga}_{1-x}\text{Al}_x\text{As}$ sawtooth superlattice with $x_{\max}=0.2$. E_g is the band gap of bulk GaAs.

We consider that the structure is in the electric quantum limit (EQL), i.e., only the ground conduction and valence subbands are occupied. The corresponding wave functions which are shown in Fig. 1 clearly present different spatial extension. This local polarization induces an overall potential difference ΔV across the structure. If the electron (hole) wave functions centered in neighboring quantum wells do not significantly overlap, we can treat each cell separately.

This unit cell consists of electron and hole quasibidimensional gases presenting distinct spatial localization. The potential difference ΔV across the superlattice is equal to the sum of local potential differences Δv between the planes $z=z_n$ and $z=z_{n+1}$ limiting the nth unit cell:

$$\Delta V=N\Delta v \tag{7}$$

and

$$\Delta v=\frac{en_s}{\epsilon\epsilon_0}\int_{z_n}^{z_{n+1}}dz\int_{z_n}^{z}dz'[\,|\psi_e^0(z')|^2-|\psi_h^0(z')|^2]\,. \tag{8}$$

N is the number of cells and ϵ the relative dielectric constant, n_s is the density of injected carriers, and $\psi_{e(h)}(z)$ is the electron (hole) ground wave function, which we take as completely confined between z_n and z_{n+1}. The boundary condition implicit in Eq. (8) ensures that the electric field vanishes outside a two-dimensional dipolar charge distribution.

Clearly, the system may be considered as a series of

capacitors corresponding to each period with the positive layer located at the z mean value of the hole wave function $\langle z_h \rangle$, and the negative layer at the z mean value of the electron wave function $\langle z_e \rangle$. Indeed, one verifies that if the wave functions are normalized in the z_n, z_{n+1} segment, the integral in Eq. (8) may be written as

$$-\int_{z_n}^{z_{n+1}} dz\, z[\,|\psi_e^0(z)|^2 - |\psi_h^0(z)|^2] = \langle z_h \rangle - \langle z_e \rangle . \quad (9)$$

Therefore

$$\Delta v = (n_s S e)\frac{(\langle z_h \rangle - \langle z_e \rangle)}{\epsilon_0 \epsilon S} = Q/C , \quad (10)$$

where S is the sample area. Δv appears as the voltage across the individual capacitor of thickness $\langle z_e \rangle - \langle z_h \rangle$. In fact, even if the wave functions have some extension in adjacent cells, the series of capacitors will remain a sensible approximation.

We consider the sawtooth superlattice with the parameters used in Ref. 1: $N=10$, $d=500$ Å, $x_{\max}=0.2$, and $\epsilon=14$. Using the wave functions calculated above, we obtain a voltage drop across the structure of $|\Delta V| \simeq 3.1-31$ mV for n_s ranging from 10^{10} to 10^{11} cm^{-2}. This agrees in order of magnitude with the measured voltage ($\Delta V \simeq 10$ mV).[1] The corresponding charge separation $\langle z_e \rangle - \langle z_h \rangle$ is equal to 26 Å.

However, one should inquire about the possible band-bending effect due to the photocarriers themselves. As a next step, we consider these effects by solving the Schrödinger and Poisson equations self-consistently. For the sake of commodity, this was done using a variational method with a modified[6] Fang-Howard function[7] as the trial wave function. Although this variational method gives a good description of the energy levels ($\approx 10\%$) the calculated wave functions are less satisfactory. This in turn affects the calculated ΔV, even when the band-bending effect is neglected: we obtain 1.4–14 mV for the example described above. However, it is still useful to examine the effects of the band-bending in the system. In the EQL, the self-consistent calculations gives, for the same parameters as used before, a photovoltage $|\Delta V| = 1.3-10$ mV. Thus, although the band bending should be taken into consideration for a refined analysis, it is not fundamental for the physical understanding of the problem as the confinement effects remain essentially unchanged.

The photovoltaic effect described above is induced by the charge separation and the lack of overall z symmetry. Type-II systems, like InAs-GaSb superlattices, present a strong spatial separation of the electron and hole wave functions. Consider a globally nonsymmetric structure, i.e., an InAs-GaSb superlattice with the same number N of InAs and GaSb layers. If we neglect the evanescent parts of the electron and hole wave functions in their respective barriers, the simple "capacitor-approximation" applies. The symmetry of the electron (hole) ground-state wave function gives $\langle z_e \rangle$ ($\langle z_h \rangle$) at the center of the InAs (GaSb) layer. Thus

$$\Delta V = \frac{N e n_s d}{2\epsilon\epsilon_0} . \quad (11)$$

For the sake of comparison, we take the same parameters as for the sawtooth superlattices ($n_s \simeq 10^{10}-10^{11}$ cm^{-2} and $d=500$ Å). We get $\Delta V = 32-320$ mV. The large quantitative difference arises from the more effective spatial separation of the carriers in type-II superlattices.

In fact, due to the absorption of light, the density of the injected carrier is not homogeneous throughout the structure. The effect of absorption may be described in a simple way: The intensity of the incoming beam decreases by a factor $e^{-\alpha d}$ in each period, and the density of injected carriers is proportional to the absorbed intensity. Thus, we get

$$\Delta V = \frac{e n_s d}{2\epsilon\epsilon_0}\left[\frac{1-e^{-N\alpha d}}{1-e^{-\alpha d}}\right] . \quad (12)$$

α is usually of the order of 5×10^{-3} to 5×10^{-2},[8] so that the photovoltaic effect saturates for a 50 to 200 period superlattice (SL). Note that absorption may supply the necessary global inversion asymmetry already mentioned.

Other structures which present equivalent properties are the *nipi* superlattices, in which the superpotential is obtained from modulation doping.[9] In these systems, injection considerably affects the SL band structure and self-consistency becomes essential. For weak injection, we expect a behavior similar to that of type-II superlattices. For large injection rates, the superpotential will be washed out and the photovoltage should decrease to zero.

Until now, we have described the quantum origin of the photovoltage. However, this effect cannot be observed under cw illumination due to the conductance parallel to

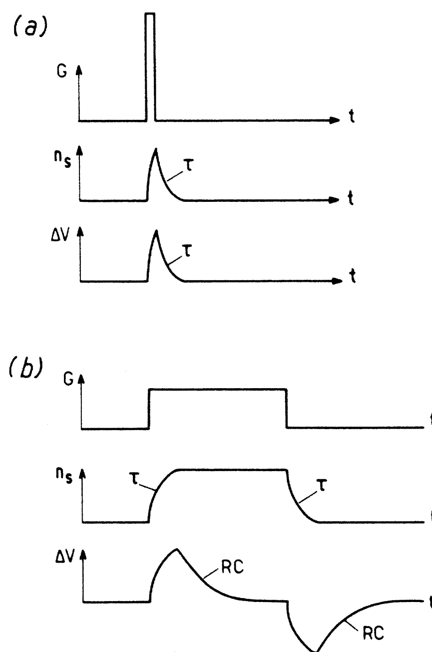

FIG. 3 Schematic representation of the time dependence of the light pulse (or pair generation rate) G, photoinjected carrier concentration n_s, and photovoltage ΔV in a transient photovoltage device when (a) $T \gg RC \gg \tau$ and (b) $T < \tau \ll RC$. T is the light pulse duration, τ and RC are defined in the text.

the growth axis. In fact, we are dealing with a transient effect governed by the RC constant of the system and the electron-hole recombination time, τ.

The carrier density n_s and the photovoltage ΔV obey the following rate equations:

$$\frac{dn_s}{dt}=G-\frac{n_s}{\tau}\ , \quad (13)$$

$$\frac{d\Delta V}{dt}=\frac{4\pi eN}{\epsilon\epsilon_0}(\langle z_h\rangle-\langle z_e\rangle)\frac{dn_s}{dt}-\frac{\Delta V}{RC}\ , \quad (14)$$

where G is the pair generation rate.

The recombination time, which is typically less than 1 ns,[7] governs the carrier concentration in the "bulk" of the sample. At the opposite, the RC constant of the system describes the relaxation of the photovoltage through a net charge transfer between the terminating planes of the structure. This RC constant may arise from the conduction of the sample parallel to the axis or be imposed by the external circuit; it may vary from the subnanosecond range to the microsecond range. In Fig. 3 we represent schematically the behavior of the photocarrier concentration and the photovoltage in function of time in the case $\tau \ll RC$ for two-pulse durations T: (i) $RC \gg \tau \gg T$ [Fig. 3(a)] and (ii) $T \gg RC \gg \tau$ [Fig. 3(b)]. In the first case, the photovoltage increases rapidly during the pulse duration and then relaxes to zero with the carrier density. All this happens before any global charge transfer has occurred. At the opposite, in the case of long pulses, the photovoltage first rises rapidly until n_s reaches the saturation value $n_s=G\tau$, then relaxes to zero through charge accumulation at the extremities of the sample. When the illumination is set to zero again, the carrier density rapidly relaxes to zero through recombination, leaving behind the charges at the extremities of the sample. The corresponding voltage has the sign opposite to the initial photovoltage. It then relaxes to zero with a slow RC constant.

If, however, we have the opposite situation, $RC \ll \tau$, we shall observe no photovoltage, independently of the illumination conditions, since the system in this case is essentially a conductor.

In conclusion, we have described theoretically a new photovoltaic effect which occurs in superlattice structures presenting the property of the spatial separation of the conduction and valence wave function. This effect may lead to the realization of interesting fast-pulse photodetectors.

One of us (J.A.B.) would like to express his gratitude to the Conselho Nacional de Desenvolvimento Científico e Tecnológico (CNPq), Brazil, for financial support. The Groupe de Physique des Solides de l'Ecole Normale Supérieure is "Laboratoire associé are Centre National de la Recherche Scientifique," France.

[1]F. Capasso, S. Luryi, W. T. Tsang, C. G. Bethea, and B. F. Levine, Phys. Rev. Lett. **51**, 2318 (1983).
[2]E. O. Göbel, H. Jung, J. Kuhl, and K. Ploog, Phys. Rev. Lett. **51**, 1588 (1983).
[3]G. Bastard, Phys. Rev. B **24**, 5693 (1981).
[4]R. C. Miller, D. A. Kleinman, and A. C. Gossard, Phys. Rev. B **29**, 7085 (1984); M. H. Meynadier, C. Delalande, G. Bastard, M. Voos, F. Alexandre, and J. L. Liévin, Phys. Rev. B **31**, 5539 (1985).
[5]M. Jaros, K. B. Wong, and M. A. Gell, Phys. Rev. B **31**, 1205 (1985).
[6]G. Bastard, Surf. Sci **142**, 284 (1984).
[7]F. F. Fang and W. E. Howard, Phys. Rev. Lett. **16**, 797 (1966).
[8]P. Voisin, in *Lecture Notes of Les Houches Winter School on Semiconductors, Heterojunctions and Superlattices, March, 1985* (Springer, New York, in press).
[9]See, for example, G. H. Döhler, J. Vac. Sci. Technol. B **1**, 278 (1983).